Title

An estimation of the main wetting branch of the soil water retention curve based on its main drying branch using the machine learning method

Journal

Water Resources Research, 53(2)

ISSN

0043-1397

Authors

Lamorski, Krzysztof
Šimůnek, Jiří
Sławiński, Cezary
et al.

Publication Date

2017-02-01

DOI

10.1002/2016wr019533

Peer reviewed

AGU PUBLICATIONS

Water Resources Research

RESEARCH ARTICLE
10.1002/2016WR019533

Key Points:
- The main wetting branch of the soil water retention curve is estimated based on its main drying branch
- The machine learning method is used for analysis
- Results are compared with classical methods of estimating the main wetting branch

Supporting Information:
- Supporting Information S1
- Data Set S1

Correspondence to:
K. Lamorski,
k.lamorski@ipan.lublin.pl

Citation:
Lamorski, K., J.ř Šimůnek, C. Sławiński, and J. Lamorska (2017), An estimation of the main wetting branch of the soil water retention curve based on its main drying branch using the machine learning method, *Water Resour. Res.*, *53*, doi:10.1002/2016WR019533.

Received 19 JUL 2016
Accepted 28 JAN 2017
Accepted article online 3 FEB 2017

An estimation of the main wetting branch of the soil water retention curve based on its main drying branch using the machine learning method

Krzysztof Lamorski[1], Jiří Šimůnek[2], Cezary Sławiński[1], and Joanna Lamorska[3]

[1]Institute of Agrophysics, Polish Academy of Sciences, Lublin, Poland, [2]Department of Environmental Sciences, University of California Riverside, Riverside, California, USA, [3]Institute of Agricultural Sciences, State School of Higher Education in Chełm, Chełm, Poland

Abstract In this paper, we estimated using the machine learning methodology the main wetting branch of the soil water retention curve based on the knowledge of the main drying branch and other, optional, basic soil characteristics (particle size distribution, bulk density, organic matter content, or soil specific surface). The support vector machine algorithm was used for the models' development. The data needed by this algorithm for model training and validation consisted of 104 different undisturbed soil core samples collected from the topsoil layer (A horizon) of different soil profiles in Poland. The main wetting and drying branches of SWRC, as well as other basic soil physical characteristics, were determined for all soil samples. Models relying on different sets of input parameters were developed and validated. The analysis showed that taking into account other input parameters (i.e., particle size distribution, bulk density, organic matter content, or soil specific surface) than information about the drying branch of the SWRC has essentially no impact on the models' estimations. Developed models are validated and compared with well-known models that can be used for the same purpose, such as the Mualem (1977) (M77) and Kool and Parker (1987) (KP87) models. The developed models estimate the main wetting SWRC branch with estimation errors (RMSE = 0.018 m^3/m^3) that are significantly lower than those for the M77 (RMSE = 0.025 m^3/m^3) or KP87 (RMSE = 0. 047 m^3/m^3) models.

1. Introduction

Soil water retention curves (SWRCs) are one of the most important soil hydrological characteristics required for both agricultural and environmental research related to the vadose zone. SWRCs link the soil water content with the soil water potential and represent indispensable information for the modeling of soil water flow processes. Although laboratory measurements are the ultimate source of information about retention curves, for many reasons SWRCs are commonly estimated using various statistical models, such as the so-called pedotransfer functions (PTF) [e.g., *Vereecken et al*., 1989, 2016; *Schaap et al*., 2001]. The main reason for using PTF estimations of SWRCs instead of direct measurements is their long duration and high cost. Typical steady state equilibrium measurements of the retention curve for a full range of soil water potentials can last several months.

PTFs estimate SWRCs based on various physical and chemical soil characteristics. For example, particle size distribution and dry bulk density are commonly used predictor variables in PTFs. Additional soil variables such as organic carbon content, soil-specific surface area, and/or cation exchange capacity can also be used. There were numerous PTF models developed utilizing different statistical and/or soft computing methods for SWRC estimation. Early PTFs were often developed using statistical regression [*Rawls et al*., 1982; *Vereecken et al*., 1989; *Wösten et al*., 1999; *Walczak et al*., 2006], leading to some still often used models. Various soft computing methods of statistical inference such as artificial neural networks (ANN) [*Schaap et al*., 2001; *Jana et al*., 2008], the *k*-nearest neighbors algorithm (*k*-NN) [*Nemes et al*., 2006; *Botula et al*., 2013], regression trees [*Tóth et al*., 2012, 2015], or support vector machines (SVM) [*Lamorski et al*., 2008] were used later on.

Soil water retention curves of many soil materials exhibit hysteretic behavior, which means that the dependence between the soil water potential (h) and the soil water content (θ) is not unique and depends on the

history of soil water content changes. As a result, soil can exhibit an interval of soil water contents for a single soil water potential. Under natural conditions, available states in the θ-h space are limited by the so-called main drying and main wetting curves. The main wetting and drying curves are obtained when the SWRC is measured starting at zero or full saturations, respectively. Since most laboratory methods for SWRC measurements determine the main drying branch, existing PTFs usually produce values for the main drying branch as well. However, for many modeling applications, it is advisable to consider hysteresis, and thus necessary to also know the main wetting branch of the SWRC. Only when both wetting and drying branches of the SWRC are known can numerical models consider soil hysteresis and determine actual values of soil water content for given values of soil water potential, taking into account historical values of soil water potential.

Hysteresis in the SWRC affects many vadose zone flow processes, often with practical implications. For example, the influence of hysteresis on runoff predictions in catchments was demonstrated by *Mirus* [2015]. Other studies showed that hysteresis influences slope stability, and neglecting it can lead to an underestimation of landslide conditions [*Ebel et al*., 2010; *Bordoni et al*., 2015]. Consideration of SWRC hysteresis in vadose zone transport modeling has an influence on soil water flow [*Trpkošová and Mls*, 2010; *Ma et al*., 2011] and solute transport [*Vereecken et al*., 1995] modeling results, especially in the upper soil layer and in the rhizosphere [*Elmaloglou and Diamantopoulos*, 2009; *Carminati et al*., 2010]. On the other hand, the effects of soil heterogeneity may overshadow the effects of hysteresis on soil water flow processes [*Vereecken et al*., 1995].

Physical phenomena which result in SWRC hysteresis [*Bachmann and van der Ploeg*, 2002; *Albers*, 2014] include (a) an ink-bottle effect due to irregular shapes of pores, (b) hysteresis of the interface contact angle, i.e., the difference between ascending and descending contact angles, (c) a rain drop effect, i.e., air bubble entrapment or Haines jumps, and (d) temporal nonequilibrium due to fast pore filling events. The research into SWRC hysteresis is still under active development, and different modeling approaches have been developed to understand or predict the SWRC hysteretic behavior. Two main modeling methodologies can be distinguished: physically based models and phenomenological models.

Physically based models take into account soil water interactions. These models focus on real physical phenomena that occur at the level of soil pores and that together with soil structure influence unsaturated soil hydrological properties [*Mahmoodlu et al*., 2016]. Real representations of pore spaces obtained from computed microtomography scanning (μCT) [*Ahrenholz et al*., 2008] or equivalent pore network models [*Joekar-Niasar et al*., 2013; *Arroyo et al*., 2015; *Rostami et al*., 2015] and individual phenomena leading to the hysteresis effect such as contact angle hysteresis [*Zhou*, 2013] or soil-water interactions and pore morphology [*Chan and Govindaraju*, 2011; *Gan et al*., 2013] are used and analyzed in these models. While these models provide insight into various physical factors leading to hysteresis, their practical applications are very limited since they are very complicated and often dependent on hard-to-get input data.

Phenomenological models are based, on the other hand, on simplified assumptions regarding the soil medium and/or on the general Everett's domain hysteresis theory. The first attempt to apply the domain theory to soil moisture hysteresis was the independent domain model of *Poulovassilis* [1962]. The similarity hypothesis for the distribution of geometrical menisci curvatures for drying/wetting relationships was introduced by *Philip* [1964], which allowed for the reduction of information needed to describe the hysteretic process to only the main wetting and drying branches. The similarity concept was further developed by *Mualem* [1973, 1984], who stated that the domain model for the water distribution function can be expressed as a simple product of two functions, one solely dependent on wetting and the other only on drying soil water potential. Another approach, which is based on a scaling hypothesis that assumes a simple dependence between main and scanning curves, was proposed by *Scott et al*. [1983]. This approach is equivalent to the Mualem model based on the similarity hypothesis. The *Scott et al*. [1983] model was then adopted for SWRCs described using the *van Genuchten* [1980] analytical function [*Kool and Parker*, 1987; *Parker and Lenhard*, 1987]. The *van Genuchten* [1980] model has been recently extended to take into account deformation of soil pores due to swelling effects [*Gallipoli*, 2012]. Another approach to describing the main and scanning curves is to define them indirectly, such as using different tangent inclinations dependent on suction [*Pedroso and Williams*, 2010]. The scanning curves can then be determined by integrating a differential equation introduced to describe the shapes of the curves. A comprehensive review of these types of models of hysteresis was recently provided by *Pham et al*. [2005] and *Albers* [2014].

Phenomenological models are still being further improved by taking into account additional multiple effects or phenomena [*Rudiyanto et al*., 2013, 2015]. Phenomenological models are very important for the soil water modeling practice because they allow for simple and easy-to-incorporate approaches for describing the hysteretic behavior of soils based on standard soil water retention information.

Most hysteretic retention models are based on information about the main drying and wetting branches of SWRCs. However, laboratory measurements of the main wetting branch of the SWRC are rarely made during soil surveys, and usually, only the main drying branch of SWRC is measured. It is thus necessary to somehow estimate the main wetting branch when the soil hysteretic behavior is to be considered; some classical models of the soil water hysteresis allow for that. For example, the universal domain model estimates hysteretic SWRCs, including the main wetting branch, based only on information about the main drying branch [*Mualem*, 1977]. *Kool and Parker* [1987] suggested an approximate method for the estimation of the main wetting branch of the SWRC parameterized using the *van Genuchten* [1980] function based on parameters of the main drying branch. Other models need additional information regarding the main wetting branch, such as the water entry value [*Hogarth et al*., 1988] or two points measured on the wetting branch [*Pham et al*., 2003]. Despite the fact that these models give a more accurate estimation [*Pham et al*., 2005] of the wetting branch of a SWRC, their practical applications are cumbersome due to prohibitive requirements on additional input data characterizing the main wetting branch of a SWRC.

The aim of this work is to develop a statistical model that will allow for the estimation of the main wetting branch of a SWRC based on knowledge of the main drying branch of the SWRC, while also providing the option to take additional information about soil physical characteristics into account. The technique of support vector machines will be used to develop this model.

2. Materials and Methods

2.1. Soil Material

Measured soil retention data are needed for the development and validation of SWRC estimating models. In this study, 104 different undisturbed soil core samples collected from the top soil layer (A horizon) of different soil profiles in Poland were analyzed (Figure 1). Standard 100 cm^3 (a 5 cm diameter) sampling rings were used in the analysis. Soils were selected to be representative of the entire country (Poland) and were a subset of the Soil Databank of Arable Mineral Soils of Poland [*Bieganowski et al*., 2013a]. Soils were mainly classified as Haplic Luvisols and Eutric Cambisols, i.e., the two main soil types in Poland. Mollic Gleysols, Eutric Fluvisols, Haplic Phaeozems, Distric Fluvisols, Rendzic Leptosols, and Terric Histosols were also represented.

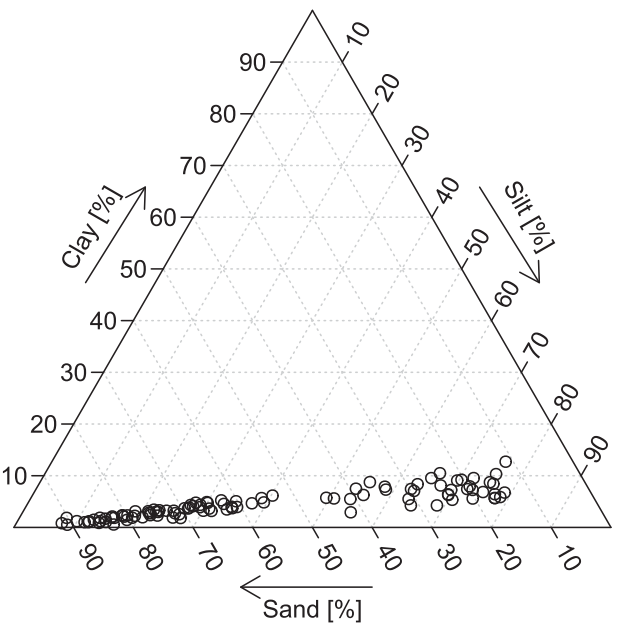

Figure 1. Textural distribution (PSD was determined by LDM) of the soil samples used in this work.

Drying and wetting branches of the SWRC were determined during a 3 year long campaign of laboratory measurements. Soil cores were initially saturated with water and then subjected to drying; the drying branch of the SWRC was measured first and the wetting branch was determined afterward starting from a soil water potential of −1554.78 kPa, which was reached at the end of the drying phase. Soil water contents were determined for seven values of a soil water potential of −3.1, −9.81, −15.54, −49.16, −155.47, −491.66, and −1554.78 kPa for the drying branch and for six values of a soil water potential of −1554.78, −310.21, −98.1, −15.54, −9.81 and −3.90 kPa for the wetting branch. Sandboxes and the hanging water column method were

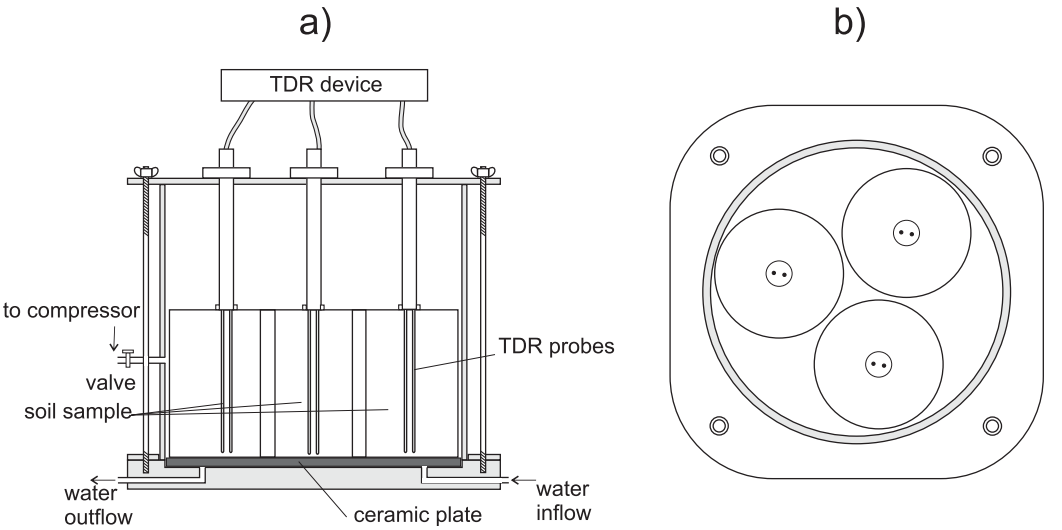

Figure 2. Schematic of the measurement cell: (a) a side view and (b) a top view.

used for soil water potentials higher than or equal to −9.81 kPa, while pressure chambers were utilized for lower potentials. The drying branch of SWRC was measured using the standard ceramic plate extractors (by Soilmoisture Equipment Corp.), which allowed for the soil water potential to be only reduced between subsequent measurements, as water could only be released from the measurement system.

For the determination of the wetting branches of the retention curves, different pressure chambers were used, which allowed for wetting of measured soil cores through the chamber ceramics between subsequent measurements. For that purpose, modified Soilmoisture Equipment volumetric pressure plate extractors (Product #1250) were used. The system was originally designed to measure changes in the soil water contents of the samples based on the extracted/applied soil water volume measured by burette. This system was adapted so that TDR probes [*Skierucha et al*., 2012a, 2012b] could be used to directly measure the soil water content in the samples (see Figure 2) rather than derive it from burette measurements. In the new setup, the TDR probes were vertically installed in the soil samples from the top, and such a TDR placement and the validity of their measurements were experimentally verified [*Pastuszka et al*., 2014]. In addition to making measurements easier, this modification also allowed us to place three soil samples in each chamber (the original system allowed only one soil core in a pressure chamber), which allowed for the simultaneous determination of the drying branches of 21 soil cores using seven pressure chambers.

In addition to SWRCs, other soil physical characteristics were determined including dry bulk density (BD), particle size distribution (PSD), which was measured using the laser diffraction method (LDM), the total organic carbon (OC), which was measured using high-temperature catalytic oxidation using TOC-VPCH (Shimadzu), and soil specific surface (SSS), which was determined using the water vapor adsorption method. The soil samples were initially sieved through the 2 mm sieve for PSD, OC, and SSS determination.

A Malvern Mastersizer 2000 with a measurement range of 0.02 μm to 2 mm was used for PSD determination. For obtaining homogeneity in the measured soil suspension, a Hydro G dispersion unit was used [*Sochan et al*., 2012]. The pump speed was 1750 rpm, and the stirrer speed was 700 rpm. The soil sample was dispersed by ultrasonication, and the power of the probe was 35 W with the time interval equal to 4 min. Light intensity measured on the detectors was recalculated into PSD according to the Mie theory (ISO 13320:2009, 2009). The Mie model parameters were an absorption coefficient of 0.1 and a refractive coefficient of 1.52 [*Bieganowski et al*., 2013b]. For each soil, the PSD curve was determined as an average value of three replications. Soil samples were not pretreated in any way before the LDM measurement.

The soil specific surface (SSS) area was determined for samples initially dried at 105°C for 24 h. The adsorption and desorption isotherms of water vapor were determined using the Dynamic Vapor Sorption-Intrinsic

Table 1. Statistical Properties of the Entire Soil Data Set[a]

Statistic	Mean	St. Dev.	Min	Max
BD (g/cm^3)	1.395	0.143	1.02	1.76
Sand (%)	55.802	25.45	11.28	91.572
Silt (%)	39.695	23.119	7.615	78.818
Clay (%)	4.504	2.638	0.518	12.713
OC (%)	1.87	0.799	0.722	5.547
SSS (m^2/g)	17.617	12.911	3.14	80.46

[a]BD, bulk density; OC, organic carbon; SSS, specific soil surface; Sand, Silt, and Clay are percentages of particular particle sizes.

(Surface Measurement Systems Ltd., UK) for a relative humidity from 0 to 100% at 20°C. The BET model was used for the determination of SSS based on desorption isotherms [*Brunauer et al*., 1938].

While the data set collected for this study is relatively large (104 soil samples), all measurements were carried out with the same experimental methodology. Such a data set, which could be used for the analysis of hysteresis, is rather unique, as most similar studies usually rely on much smaller data sets or data sets collected from different sources. An overview of descriptive statistics for the soil data set is presented in Table 1.

2.2. SWRC Data Pretreatment

Laboratory measurements provided information about the drying and wetting branches of SWRCs in the form of measured pairs of soil water contents and soil water potentials. The soil hydraulic parameters of the van Genuchten (vG) function were fitted to both drying and wetting branches of SWRCs for all soil samples. An assumption was made that both branches had the same residual and saturated water contents. For fitting of the vG model's parameters, a custom script was written in R language that was based on the Nelder-Mead minimization of RMSEs (root-mean-square errors) between measured and vG model predicted soil water contents for given soil water potentials.

2.3. SVM SWRC Modeling

The support vector machines approach (SVM), one of many algorithms among machine learning methodologies, was selected for the SWRC model development. The SVM approach has been previously used in subsurface hydrology for facies delineation [*Tartakovsky and Wohlberg*, 2004; *Wohlberg et al*., 2006], SWRC modelling [e.g., *Lamorski et al*., 2008; *Twarakavi et al*., 2009], or for predictions of time-variable soil water contents [e.g., *Lamorski et al*., 2013; *Karandish and Šimůnek*, 2016]. While SVM was originally developed for solving classification problems, its usage has later been extended to regression-type problems [*Vapnik*, 1995]. When used for regression modeling, SVM estimates one output variable based on a set of independent input variables. Since SVM is a supervised learning method, it requires a training data set for the model's development. The resulting model reproduces input-output relationships present in the training data set and is able to make estimations for any values of input variables. A model based on a training data set is subject to validation based on a testing data set. SVM models, similarly like ANN or *k*-NN-based models, have to be developed and used by means of software because their final form is not a simple, explicit relationship. In this study, the R statistical computing environment was used for that purpose.

Support vectors (SV), a kernel function, and model parameters are selected during the SVM model development and together constitute the model. The core of the SVM model are so-called support vectors (SV), which are a subset of a training data set, thoroughly selected during the model development procedure. There is a strict dependence between the number of SVs and the generalization capability of the model. An optimal number of SVs is about half of a training data set. Incorporating more SVs in the model will lead to overtraining, i.e., model estimations will be very good for a training data set, while estimation errors will be very high for a testing data set [*Lamorski et al*., 2014].

The SVM methodology used in this paper was previously applied for the development of pedotransfer functions (PTF) for the estimation of SWRCs by *Lamorski et al*. [2014], in which all details can be found. The ν-SVM algorithm was used for the estimation of SWRCs. SVM rely on a selectable model component, the so-called kernel function; a radial basis kernel function was used in the study of *Lamorski et al*. [2014]. The model parameters were searched for using the genetic algorithm optimization technique. The objective function that was used in this process was based on RMSE between measured and estimated SWRC, while also explicitly taking into account the number of support vectors used in the developed model. The use of such an objective function instead of one only based on RMSE avoids overtraining during the model development.

Table 2. Names and Definitions of SVM Models[a]

Model Name	Input Variables	Estimation Method
$M0_d$	SWRC	Direct
$M0_p$		Parametric
$M1_d$	SWRC, BD	Direct
$M1_p$		Parametric
$M2_d$	SWRC, BD, Sand, Silt, Clay	Direct
$M2_p$		Parametric
$M3_d$	SWRC, BD, Sand, Silt, Clay, OC	Direct
$M3_p$		Parametric
$M4_d$	SWRC, BD, Sand, Silt, Clay, OC, SSS	Direct
$M4_p$		Parametric

[a]A list of variables considered by the estimation methods of different SVM models.

2.4. SVM Model Development

The soil data set was randomly divided into the training (78 soils) and testing (26 soils) data sets for the SVM model development. Five different types of models (M0 through M4) were developed based on the regression analysis of available soil data. While all five models allowed for the determination of the wetting branch of SWRC, they used different sets of input parameters. All models used information about the drying branches of SWRCs. All models, except for M0, used additional soil characteristics as input parameters (i.e., PSD, BD, OC, and SSS; see Table 2). Soil physical parameters were included as input for the developed models since they were correlated with the wetting branch of SWRC, and thus their inclusion into the analysis could have a positive impact on model estimations.

SWRC data were either directly (subscript *d*) or parametrically (subscript *p*) considered in each SVM model. In both cases, the first step was to fit the van Genuchten model to measured retention data points. In the direct approach, 15 soil water contents evaluated from the van Genuchten functions fitted to the drying branches of SWRCs for the following soil water potentials were considered: −0.00981, −0.031, −0.0981, −0.310, −0.981, −3.102, −9.81, −15.547, −31.021, −49.166, −98.1, −155.478, −310.21, −491.664, and −1554.780 kPa. The direct models estimated soil water contents for the wetting branches of SWRCs for the same set of soil water potentials. In the parametric models, SWRC input information was represented using the van Genuchten parameters fitted to the drying branches of SWRCs. Similarly, the parametric models estimated the vG parameters of the wetting branches of SWRCs. Altogether, 10 different SVM models were constructed and validated (see Table 2).

Both direct and parametric approaches for the model development were considered here since there is still an ongoing discussion regarding the best SWRC modeling methodology. While some researchers report better accuracy of the direct approach [*Schaap*, 2004; *Børgesen and Schaap*, 2005], others reported no differences between direct and parametric approaches [*Merdun*, 2006].

2.5. Models' Cross Validation

Different cross-validation techniques can be utilized to assess the quality of the developed models and their selected parameters when the data learning concept is used [*Hastie et al*., 2009]. The *k*-fold cross validation was used for that purpose in this study. The training data set, which was used for model development and consists of 78 soil data records, was randomly divided into five disjunctive subsets (i.e., folds), with 15 or 16 soil data records in each subset (fold 1–16, fold 2–16, fold 3–16, fold 4–15, fold 5–15). The folds used for data preparation were sequentially rotated five times, which allowed for the preparation of five sets of data, which were then used for model development. Five training data sets were set up, each with four joined folds (62 or 63 samples). One SVM submodel was then created for each of the five different training data sets. The resulting final models, which were developed using the *k*-fold method, estimate water contents as an average outcome from the five submodels.

2.6. Classical Models for Estimating Wetting Branches of SWRCs

The wetting branch of the SWRC may be estimated using several approaches suggested in the literature [*Mualem*, 1977; *Kool and Parker*, 1987; *Hogarth et al*., 1988; *Pham et al*., 2003]. However, if only the knowledge of the drying branch of the SWRC is to be used as input information for this estimate, only two models are currently available [*Mualem*, 1977; *Kool and Parker*, 1987].

Mualem's [1977] model, which is based on the dependent-domain theory of hysteresis, is described by equation (1). This model directly relates soil water contents of the wetting branch of the SWRC with soil water contents of the drying branch of the SWRC for a given soil water potential:

$$S_w^e(h)=1-\sqrt{1-S_d^e(h)} \quad (1)$$

where h is the pressure head (m), and $S_w^e(h)$ and $S_d^e(h)$ are effective degrees of saturation for the wetting and drying branches, respectively, described by equations:

$$S_w^e(h)=\frac{\theta_w(h)-\theta_{res}}{\theta_{sat}-\theta_{res}} \quad (2)$$

and

$$S_d^e(h)=\frac{\theta_d(h)-\theta_{res}}{\theta_{sat}-\theta_{res}} \quad (3)$$

where θ_{res} and θ_{sat} are the residual and saturated water contents, respectively, and $\theta_d(h)$ and $\theta_w(h)$ are the water contents on the draining and wetting branches of the SWRC, respectively.

The model of *Kool and Parker* [1987], contrary to the model of *Mualem* [1977] that operates directly with the water contents of the drying branch of the SWRC, relates parameters of the van Genuchten parametric representation of the drying and wetting branches of the SWRC. The model of *Kool and Parker* [1987] assumes that the n parameters for the wetting and drying branches of the SWRC are the same and that the α parameters of the two branches are related as follows:

$$\alpha_w=2\alpha_d \quad (4)$$

where α_w and α_d are vG function parameters for the wetting and drying branches of the SWRC, respectively. The other vG function parameters have the same values for both wetting and drying branches of SWRC. The *Kool and Parker* [1987] model of hysteresis is, for example, implemented into the widely used vadose zone HYDRUS [*Šimůnek et al*., 2008] and SWAP [*van Dam et al*., 2008] models.

3. Results and Discussion

The developed SVM models were validated against the testing data set, which is a basic source of information about a model's quality of estimation. Additionally, estimates made by the SVM models were compared with estimates made by the alternative—literature models that allow for the estimation of the SWRC wetting branch based only on information about the SWRC drying branch. These models will be further referred to as M77 [*Mualem*, 1977] and KP87 [*Kool and Parker*, 1987].

The results presented in Table 3 indicate that there are no substantial differences between estimations made by different SVM models and that improvements obtained by the more complex SVM models with respect to R^2 or RMSE as a comparison criterion are not significant. Models $M0_d$ and $M0_p$, which only use information about the drying branches of SWRCs, have the same statistical indices as models $M1_d$ and $M1_p$,

Table 3. Statistics of Various SVM and Classical Models[a]

	R^2			RMSE		
Model Name	Value	SD	Group	Value (m^3/m^3)	SD (m^3/m^3)	Group
$M0_d$	0.984	0.02	A	0.018	0.014	A
$M0_p$	0.985	0.02	A	0.017	0.016	A
$M1_d$	0.984	0.02	A	0.018	0.015	A
$M1_p$	0.984	0.021	A	0.018	0.017	A
$M2_d$	0.986	0.017	A	0.018	0.017	A
$M2_p$	0.986	0.016	A	0.018	0.017	A
$M3_d$	0.986	0.017	A	0.018	0.018	A
$M3_p$	0.985	0.015	A	0.02	0.021	A
$M4_d$	0.985	0.017	A	0.019	0.018	A
$M4_p$	0.986	0.015	A	0.019	0.02	A
M77 [*Mualem*, 1977]	0.97	0.036	AB	0.025	0.014	AB
KP87 [*Kool and Parker*, 1987]	0.939	0.061	B	0.047	0.022	B

[a]R^2, coefficient of determination; RMSE, root-mean-square error; SD, standard deviation; Group, grouping based on the Tukey test for group mean differences. The RMSE and R^2 values for the SVM models average results obtained by five submodels generated for each fold. SDs are related to the spread of results achieved for different folds.

which additionally consider the bulk density (BD) as an independent variable for estimations. In fact, the inclusion of BD has no discernible impact on estimations. A similar observation was made by *Schaap et al*. [2001], who showed that consideration of BD in their pedotransfer functions produced better estimates only for the saturated water content, which in our study, we kept the same as for the SWRC drying branch. No improvements in estimations were also observed when PSD information was considered among input variables. Consideration of additional soil variables, such as OC or SSS, produces only a limited increase in prediction quality (Table 3).

Since consideration of other soil information, in addition to the drying branches of SWRCs, has not substantially improved SVM models' predictive capabilities, from a practical point of view, it is not necessary to use such information for the estimation of the SWRC wetting branch. This result can be interpreted in the following way. In the statistical sense, information about soil physical parameters is already taken into account and thus "hidden" in information about the drying branches of SWRCs. As a result, an explicit use of these parameters as additional input variables for the estimation of the wetting branches has no discernible impact on the results.

The developed SVM models performed better than the M77 model (Table 3), which also estimates the wetting branch of the SWRC solely based on the drying branch. Although, the differences in predictions by the SVM models and the M77 model were not significant in a statistical sense (using the Tukey test for group mean differences with a confidence level of 0.95), the RMSE for the M77 model was higher (0.025) than for the SVM models (0.018).

Significant differences (the Tukey test) in the quality of estimations of the wetting branches of SWRCs were observed (Table 3) between the SVM models and the KP87 model [*Kool and Parker*, 1987]. For the randomly selected testing data set, the RMSE for the KP87 model was about 3 times larger than for the SVM models. While *Kool and Parker* [1987] suggested the use of $\alpha_w = 2\alpha_d$, other authors proposed different relations depending on the soil type. For example, *Likos et al*. [2014], for a soil data set involving 25 samples, determined the average relation of $\alpha_w = 2.24\alpha_d$, while for subsets of cohesive soils, $\alpha_w = 1.74\alpha_d$, and cohesionless soils, $\alpha_w = 3.14\alpha_d$. A comparison of the KP87 model with our experimental data shows that this model significantly underestimates hysteresis of SWRCs and that both the SVM models and the M77 model provide better predictions. Our data further indicate that the constrains of the KP77 model, requiring the same *n* parameter for both the drying and wetting branches, are too restrictive and prevent successful application of this model to our data set.

One of the reasons for these differences may be the fact that the KP87 model [*Kool and Parker*, 1987] was proposed based on SWRC data that were only measured for a narrow range of soil water potentials between 0 cm and about −100 cm, while the measurement range for our data set was significantly larger. The other reason for relatively high KP87 model estimation errors may be the fact that for our data set, the

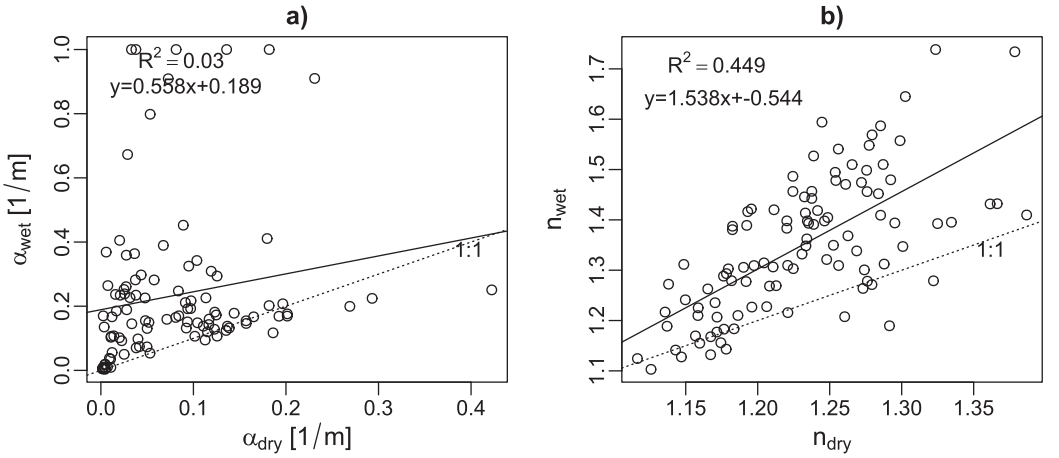

Figure 3. Comparisons between the vG parameters (a) α and (b) *n* fitted to the measured wetting and drying branches of SWRCs for the entire data set. Dotted lines represent 1:1 lines and solid lines represent linear regression lines fitted to measured and estimated water contents.

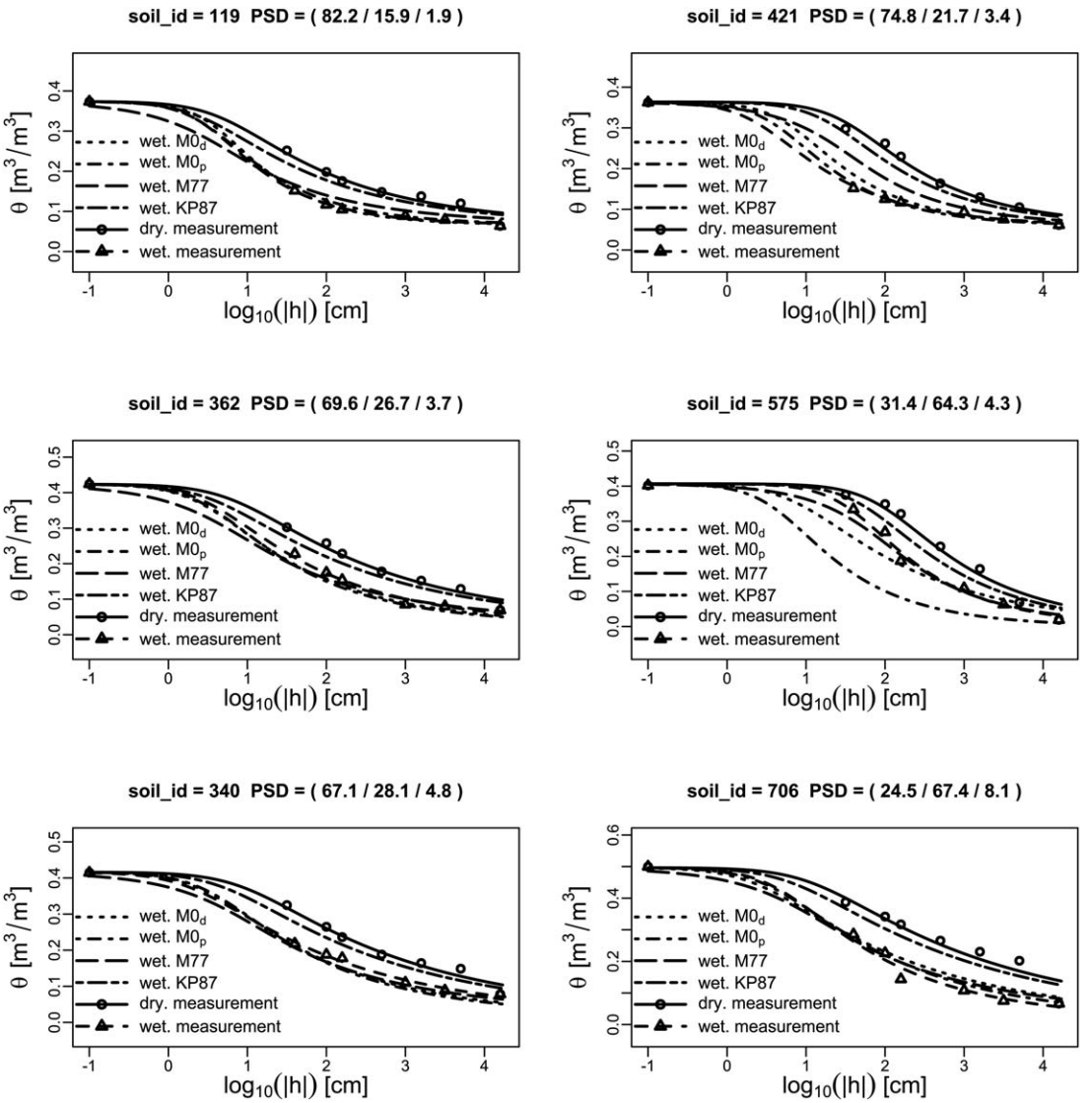

Figure 4. Comparison of measured (points) and fitted (lines) main drying ("*dry. measurement*") and wetting ("*wet. measurement*") SWRC branches for six selected soils from the testing data set. Estimated main wetting branches by direct and parametric PTFs are shown as "*wet. M0$_d$*" and "*wet. M0$_p$*" lines, respectively. Main wetting branches estimated using the method of *Mualem* [1977] and *Kool and Parker* [1987] are displayed as "*wet. M77*" and "*wet. KP87*" lines, respectively. Soil_id is the soil identification number in the database, and PSD = (sand/silt/clay) are percentages of particular particle sizes.

n parameters for wetting and related drying branches are not the same, which is an assumption of the KP87 model. In this study, both of the vG parameters α and *n* were independently optimized for the wetting and drying SWRC branches. Their dependence is displayed in Figure 3. The *n* parameter for the wetting branch is usually larger than for the drying branch, and there is a correlation between these two values ($R^2 = 0.45$). On the other hand, values of the wetting and drying α parameters are not correlated ($R^2 = 0.03$; Figure 3). The α_{wet} values are in most cases, although not all, higher than the α_{dry} values. The mean values of α and *n* parameters for the entire data set are: $<\alpha_{dry}> = 0.0789$, $<\alpha_{wet}> = 0.233$, $<n_{dry}> = 1.23$, and $<n_{wet}> = 1.35$, i.e., $<\alpha_{wet}> = 2.95<\alpha_{dry}>$. However, this ratio of α values cannot be used for estimating the wetting branch from the drying branch as is done in the KP87 model because there is no correlation between α_{wet} and α_{dry}, and thus this ratio does not express any trend between the α_{wet} and α_{dry} values.

Figure 4 shows a comparison of measured and estimated wetting and drying SWRC branches for six soils selected from the testing data set. It presents experimentally measured values of soil water contents for the drying branch of SWRCs and their fit with the vG function. Figure 4 additionally shows experimentally measured values of soil water contents for the wetting branch (dots), vG functions

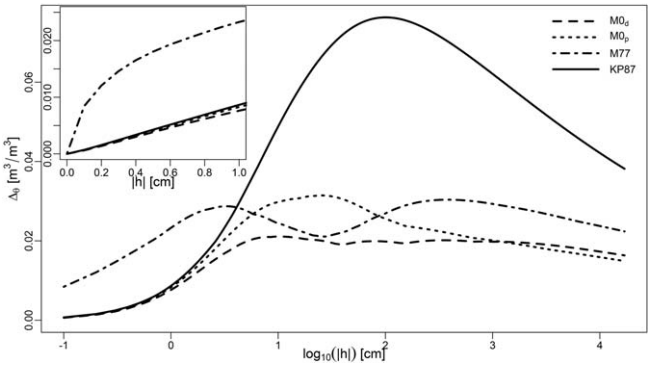

Figure 5. Mean residuals between the vG functions fitted to the measured soil water contents for the wetting SWRC branches and those estimated by different models for the testing data set.

estimated using the SVM parametric models or fitted to water contents estimated using the SVM direct models for the wetting branch of SWRCs, as well as estimations made using the KP87 and M77 models. These examples provide visual confirmations of conclusions discussed above related to Table 3.

Residuals, i.e., mean absolute values of the estimation error for the testing data set, between the vG functions fitted to the measured soil water contents of the SWRC wetting branches and vG functions estimated using the

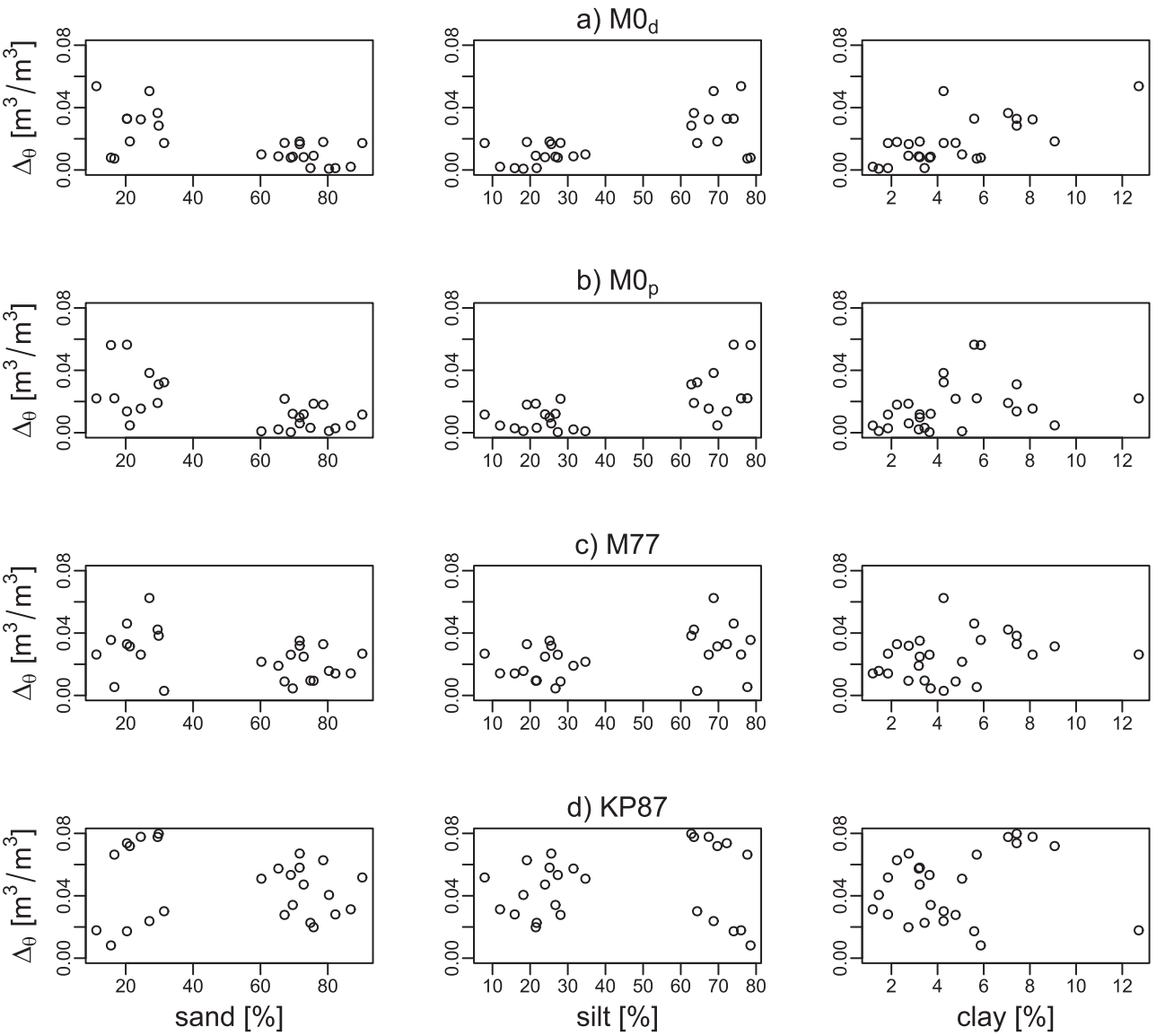

Figure 6. Scatterplots of residuals as a function of texture for different models (a) $M0_d$, (b) $M0_p$, (c) M77, and (d) KP87, used for the estimation of the wetting branches of SWRCs.

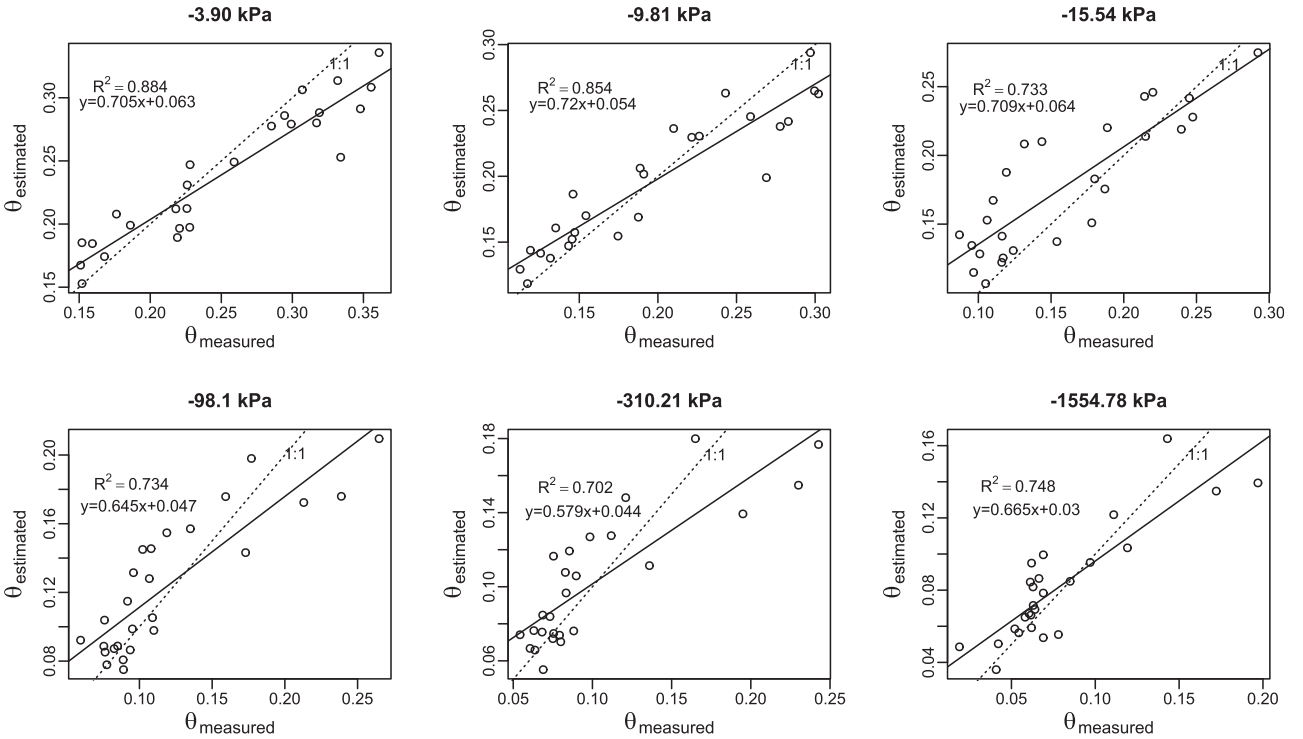

Figure 7. Comparison between measured and estimated (i.e., derived from estimated vG functions by the $M0_d$ model) soil water contents for selected soil water potentials. Dotted lines represent the 1:1 line, solid lines represent a linear regression line fitted to measured and estimated water contents.

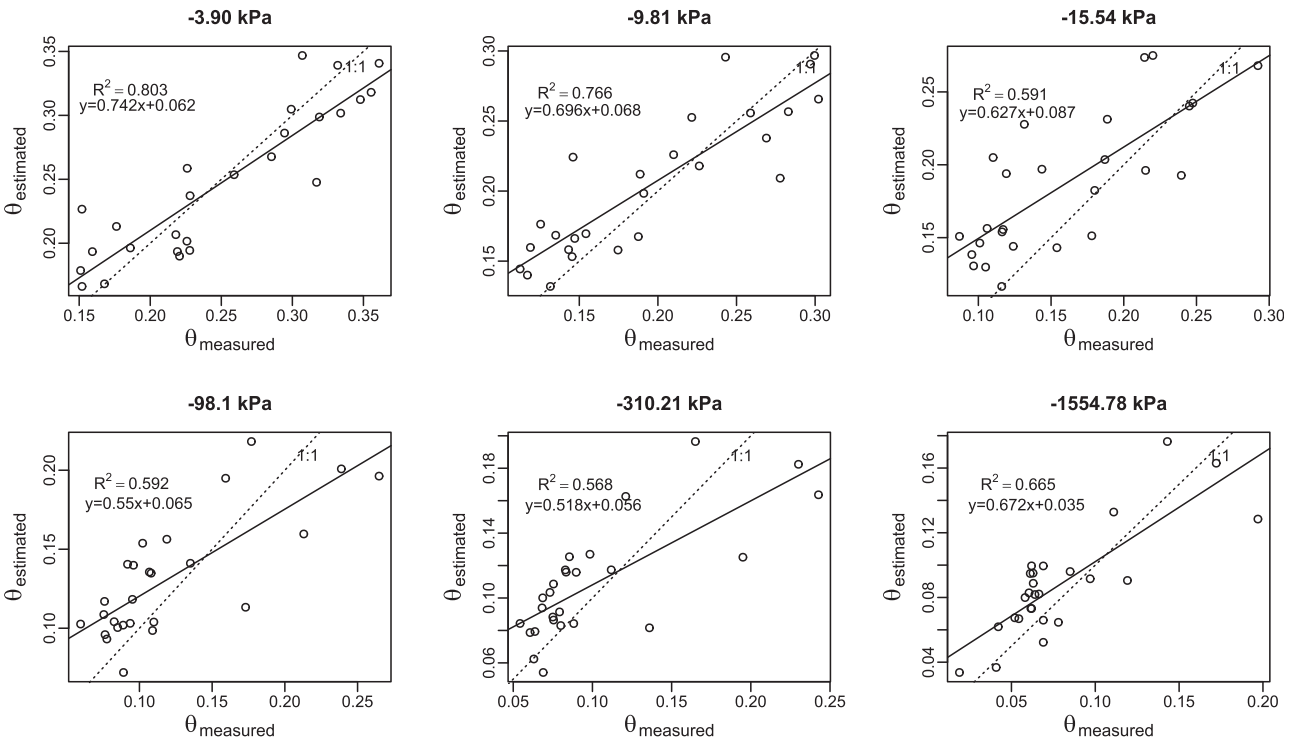

Figure 8. Comparison between measured and estimated (i.e., derived from estimated vG functions by the M77 model) soil water contents for selected soil water potentials. Dotted lines represent the 1:1 line, solid lines represent a linear regression line fitted to measured and estimated water contents.

$M0_d$, $M0_p$, M77, and KP87 models, are presented in Figure 5. The estimation errors for the KP87 model are highest almost throughout the entire interval of soil water pressure heads, except below the pressure head of ~ -5 cm where the estimation errors for the M77 model are larger. Interestingly, the M77 model has a different trend of estimation errors than the other models, especially near saturation (see subplot in Figure 5). Its estimation errors almost up to the saturation point have large values when compared to the other models. The errors of the parametric SVM model ($M0_p$) are larger than those of the direct SVM model ($M0_d$) in the range of the pressure heads from ~ -3 to ~ -300 cm.

Residuals for each soil from the testing data set were also individually analyzed using scatter plots for any possible dependency on the particle size distribution (Figure 6). One can observe a similar dependency of the $M0_p$, $M0_d$, and M77 models on texture with the estimation errors being smaller for soils with higher sand (lower silt) contents than for fine textured soils. The KP87 model does not display such dependency, and residuals are approximately in the same wide range regardless of soil texture.

The analyses of estimation errors reported so far were based on differences between the vG functions of the wetting branches of SWRCs estimated by different models and the vG fits to measured points of the wetting branches. Figure 7 shows the comparisons between measured and estimated (i.e., derived from estimated vG functions) soil water contents for selected soil water potentials. The coefficients of determination show a fairly good agreement with $R^2 \in (0.7, 0.88)$ between measured and estimated soil water contents. All fitted linear models have slopes less than 1 and small values of positive intercepts (see Figure 7), which indicates that the models underestimated water contents. The comparisons between measured and estimated (using the M77 model) soil water contents for selected soil water potentials are presented on Figure 8. The coefficients of determination between measured and estimated soil water contents $R^2 \in (0.56, 0.80)$ are slightly lower than for the SVM models, but still relatively high considering that the M77 model was not calibrated on the basis of this soil data set. In this case the results are also biased and the M77 model underestimates water contents compared to measured values of the wetting branch of SWRC.

4. Conclusions

Statistical models were developed in this study that estimate wetting branches of the soil water retention curve using the information about the routinely determined drying branch and other optional soil physical characteristics (PSD, BD, OM, or SSS). Developed models for the estimation of the wetting branch of SWRC utilize soft computing methodology that is based on the SVM algorithm. The developed models were validated against testing data, producing a good agreement between measured and estimated wetting branches of SWRCs. The RMSE was about 0.018 m^3/m^3, which compares well with typical estimation errors obtained by statistical methods used for SWRC modeling [e.g., *Schaap et al.*, 2001].

It was observed that taking soil information other than about the drying branches of SWRCs into account has essentially no impact on the models' estimations. It can be concluded that developed SVM models can estimate the wetting branches of SWRCs solely based on information about the drying branches of SWRCs. Other than the drying branches of SWRCs, consideration of any soil physical properties as model input parameters is of no use and leads only to a needless increase in model complexity. The developed $M0_d$ or $M0_p$ models may be used for most practical applications.

Two types of models were developed and validated in this study: the direct and parametric models, which either directly use SWRC data points or the van Genuchten parameters of the drying branches of SWRCs, respectively. These two approaches are alternatively used in many PTF modeling studies, and different authors advocate one of these two modeling approaches. Our results (Table 3 and Figures 5 and 6) show that there are only minor differences between the PTF models that were developed directly using SWRC data points or the van Genuchten parameters as input variables. There are no substantial differences between the parametric and direct approaches for hysteretic SWRC modeling.

The estimation errors of developed models were compared with the alternative classical models (*Mualem* [1977] or *Kool and Parker* [1987]) that can be used for the same purpose. In both cases, the new SVM-based models produced much lower estimation errors. The RMSE for the M77 model was about 1.4 times larger than for the SVM model. Much worse results were obtained using the KP87 model, which had a RMSE 2.6

larger than the SVM model. This was mainly due to the fact that the assumptions of the KP87 model were not valid for the underlying database.

However, taking into account the complexity of the SVM-based models ($M0_d$ and $M0_p$), which cannot be described explicitly, and the simplicity of the M77 model, which is described by a single equation, one may still prefer using the M77 model for practical applications.

Acknowledgments
This work has been partially supported by the National Science Centre, research grant 2011/01/B/ST10/07544. The data set used for this study is available as a supporting information or upon request from the corresponding author.

References

Ahrenholz, B., J. Tölke, P. Lehmann, A. Peters, A. Kaestner, M. Krafczyk, and W. Durner (2008), Prediction of capillary hysteresis in a porous material using lattice-Boltzmann methods and comparison to experimental data and a morphological pore network model, *Adv. Water Resour.*, *31*(9), 1151–1173, doi:10.1016/j.advwatres.2008.03.009.

Albers, B. (2014), Modeling the hysteretic behavior of the capillary pressure in partially saturated porous media: A review, *Acta Mech.*, *225*(8), 2163–2189, doi:10.1007/s00707-014-1122-4.

Arroyo, H., E. Rojas, M. de la Luz Pérez-Rea, J. Horta, and J. Arroyo (2015), A porous model to simulate the evolution of the soil–water characteristic curve with volumetric strains, *C. R. Méc.*, *343*(4), 264–274, doi:10.1016/j.crme.2015.02.001.

Bachmann, J., and R. R. van der Ploeg (2002), A review on recent developments in soil water retention theory: Interfacial tension and temperature effects, *J. Plant Nutr. Soil Sci.*, *165*(4), 468–478.

Bieganowski, A., B. Witkowska-Walczak, J. Gliński, Z. Sokołowska, C. Sławiński, M. Brzezińska, and T. Włodarczyk (2013a), Database of Polish arable mineral soils: A review, *Int. Agrophys.*, *27*(3), 335–350, doi:10.2478/intag-2013-0003.

Bieganowski, A., T. Chojecki, M. Ryzak, A. Sochan, and K. Lamorski (2013b), Methodological aspects of fractal dimension estimation on the basis of particle size distribution, *Vadose Zone J.*, *12*(1).

Bordoni, M., C. Meisina, R. Valentino, N. Lu, M. Bittelli, and S. Chersich (2015), Hydrological factors affecting rainfall-induced shallow landslides: From the field monitoring to a simplified slope stability analysis, *Eng. Geol.*, *193*, 19–37, doi:10.1016/j.enggeo.2015.04.006.

Børgesen, C. D., and M. G. Schaap (2005), Point and parameter pedotransfer functions for water retention predictions for Danish soils, *Geoderma*, *127*(1–2), 154–167, doi:10.1016/j.geoderma.2004.11.025.

Botula, Y.-D., A. Nemes, P. Mafuka, E. Van Ranst, and W. M. Cornelis (2013), Prediction of water retention of soils from the humid tropics by the nonparametric—Nearest neighbor approach, *Vadose Zone J.*, *12*(2), doi:10.2136/vzj2012.0123.

Brunauer, S., P. H. Emmett, and E. Teller (1938), Adsorption of gases in multimolecular layers, *J. Am. Chem. Soc.*, *60*(2), 309–319.

Carminati, A., A. B. Moradi, D. Vetterlein, P. Vontobel, E. Lehmann, U. Weller, H.-J. Vogel, and S. E. Oswald (2010), Dynamics of soil water content in the rhizosphere, *Plant Soil*, *332*(1–2), 163–176, doi:10.1007/s11104-010-0283-8.

Chan, T. P., and R. S. Govindaraju (2011), Pore-morphology-based simulations of drainage and wetting processes in porous media, *Hydrol. Res.*, *42*(2–3), 128–149, doi:10.2166/nh.2011.058.

Ebel, B. A., K. Loague, and R. I. Borja (2010), The impacts of hysteresis on variably saturated hydrologic response and slope failure, *Environ. Earth Sci.*, *61*(6), 1215–1225, doi:10.1007/s12665-009-0445-2.

Elmaloglou, S., and E. Diamantopoulos (2009), Effects of hysteresis on redistribution of soil moisture and deep percolation at continuous and pulse drip irrigation, *Agric. Water Manag.*, *96*(3), 533–538, doi:10.1016/j.agwat.2008.09.003.

Gallipoli, D. (2012), A hysteretic soil-water retention model accounting for cyclic variations of suction and void ratio, *Géotechnique*, *62*(7), 605–616, doi:10.1680/geot.11.P.007.

Gan, Y., F. Maggi, G. Buscarnera, and I. Einav (2013), A particle-water based model for water retention hysteresis, *Geotech. Lett.*, *3*, 152–161.

Hastie, T., R. Tibshirani, and J. Friedman (2009), *The Elements of Statistical Learning: Data Mining, Inference and Prediction*, 2nd ed., Springer, New York.

Hogarth, W. L., J. Hopmans, J.-Y. Parlange, and R. Haverkamp (1988), Application of a simple soil-water hysteresis model, *J. Hydrol.*, *98*(1–2), 21–29, doi:10.1016/0022-1694(88)90203-X.

Jana, R. B., B. P. Mohanty, and E. P. Springer (2008), Multiscale Bayesian neural networks for soil water content estimation, *Water Resour. Res.*, *44*, W08408, doi:10.1029/2008WR006879.

Joekar-Niasar, V., F. Doster, R. T. Armstrong, D. Wildenschild, and M. A. Celia (2013), Trapping and hysteresis in two-phase flow in porous media: A pore-network study, *Water Resour. Res.*, *49*, 4244–4256, doi:10.1002/wrcr.20313.

Karandish, F., and J. Šimůnek (2016), A comparison of numerical and machine-learning modeling of soil water content with limited input data, *J. Hydrol.*, *543*, 892–909, doi:10.1016/j.jhydrol.2016.11.007.

Kool, J. B., and J. C. Parker (1987), Development and evaluation of closed-form expressions for hysteretic soil hydraulic properties, *Water Resour. Res.*, *23*(1), 105–114.

Lamorski, K., Y. Pachepsky, C. Sławiński, and R. T. Walczak (2008), Using support vector machines to develop pedotransfer functions for water retention of soils in Poland, *Soil Sci. Soc. Am. J.*, *72*(5), 1243–1247.

Lamorski, K., T. Pastuszka, J. Krzyszczak, C. Sławiński, and B. Witkowska-Walczak (2013), Soil water dynamic modeling using the physical and support vector machine methods, *Vadose Zone J.*, *12*(4), doi:10.2136/vzj2013.05.0085.

Lamorski, K., C. Sławiński, F. Moreno, G. Barna, W. Skierucha, and J. L. Arrue (2014), Modelling soil water retention using support vector machines with genetic algorithm optimisation, *Sci. World J.*, *2014*, 740521, doi:10.1155/2014/740521.

Likos, W. J., N. Lu, and J. W. Godt (2014), Hysteresis and uncertainty in soil water-retention curve parameters, *J. Geotech. Geoenviron. Eng.*, *140*(4), 4013050, doi:10.1061/(ASCE)GT.1943-5606.0001071.

Ma, K.-C., Y.-C. Tan, and C.-H. Chen (2011), The influence of water retention curve hysteresis on the stability of unsaturated soil slopes, *Hydrol. Processes*, *25*, 3563–3574, doi:10.1002/hyp.8081.

Mahmoodlu, M. G., A. Raoof, T. Sweijen, and M. T. van Genuchten (2016), Effects of sand compaction and mixing on pore structure and the unsaturated soil hydraulic properties, *Vadose Zone J.*, *15*(8), doi:10.2136/vzj2015.10.0136.

Merdun, H. (2006), Pedotransfer functions for point and parametric estimations of soil water retention curve, *Plant Soil Environ.*, *52*(7), 321–327.

Mirus, B. B. (2015), Evaluating the importance of characterizing soil structure and horizons in parameterizing a hydrologic process model, *Hydrol. Processes*, *29*(21), 4611–4623, doi:10.1002/hyp.10592.

Mualem, Y. (1973), Modified approach to capillary hysteresis based on a similarity hypothesis, *Water Resour. Res.*, *9*(5), 1324–1331, doi:10.1029/WR009i005p01324.

Mualem, Y. (1977), Extension of the similarity hypothesis used for modeling the soil water characteristics, *Water Resour. Res.*, *13*(4), 773–780.
Mualem, Y. (1984), A modified dependent-domain theory of hysteresis, *Soil Sci.*, *137*(5), 283–291.
Nemes, A., W. J. Rawls, and Y. A. Pachepsky (2006), Use of the nonparametric nearest neighbor approach to estimate soil hydraulic properties, *Soil Sci. Soc. Am. J.*, *70*(2), 327–336, doi:10.2136/sssaj2005.0128.
Parker, J. C., and R. J. Lenhard (1987), A model for hysteretic constitutive relations governing multiphase flow: 1. Saturation-pressure relations, *Water Resour. Res.*, *23*(12), 2187–2196, doi:10.1029/WR023i012p02187.
Pastuszka, T., J. Krzyszczak, C. Sławiński, and K. Lamorski (2014), Effect of time-domain reflectometry probe location on soil moisture measurement during wetting and drying processes, *Measurement*, *49*(1), 182–186, doi:10.1016/j.measurement.2013.11.051.
Pedroso, D. M., and D. J. Williams (2010), A novel approach for modelling soil–water characteristic curves with hysteresis, *Comput. Geotech.*, *37*(3), 374–380, doi:10.1016/j.compgeo.2009.12.004.
Pham, H. Q., D. G. Fredlund, and S. L. Barbour (2003), A practical hysteresis model for the soil–water characteristic curve for soils with negligible volume change, *Géotechnique*, *53*(2), 293–298, doi:10.1680/geot.53.2.293.37264.
Pham, H. Q., D. G. Fredlund, and S. L. Barbour (2005), A study of hysteresis models for soil-water characteristic curves, *Can. Geotech. J.*, *42*, 1548–1568, doi:10.1139/T05-071.
Philip, J. R. (1964), Similarity hypothesis for capillary hysteresis in porous materials, *J. Geophys. Res.*, *69*(8), 1553–1562, doi:10.1029/JZ069i008p01553.
Poulovassilis, A. (1962), Hysteresis of pore water, an application of the concept of independent domains, *Soil Sci.*, *93*(6), 405–412.
Rawls, W. J., C. L. Brakensiek, and K. E. Saxton (1982), Estimation of soil water properties., *Trans. Am. Soc. Agric. Eng.*, *25*(5), 1316–1320, 1328.
Rostami, A., G. Habibagahi, M. Ajdari, and E. Nikooee (2015), Pore network investigation on hysteresis phenomena and influence of stress state on the SWRC, *Int. J. Geomech.*, *15*(5), 4014072, doi:10.1061/(ASCE)GM.1943-5622.0000315.
Rudiyanto, N. Toride, M. Sakai, and J. Šimůnek (2013), A hysteretic model of hydraulic properties for dual-porosity soils, *Soil Sci. Soc. Am. J.*, *77*, 1182–1188, doi:10.2136/sssaj2012.0339n.
Rudiyanto, M. Sakai, M. T. van Genuchten, A. A. Alazba, B. I. Setiawan, and B. Minasny (2015), A complete soil hydraulic model accounting for capillary and adsorptive water retention, capillary and film conductivity, and hysteresis, *Water Resour. Res.*, *51*, 8757–8772, doi:10.1002/2015WR017703.
Schaap, M. G. (2004), Accuracy and uncertainty in PTF predictions, in *Developments in Soil Science*, vol. 30, edited by Y. Pachepsky and W. J. Rawls, pp. 33–43, Elsevier, Amsterdam.
Schaap, M. G., F. J. Leij, and M. T. van Genuchten (2001), Rosetta: A computer program for estimating soil hydraulic parameters with hierarchical pedotransfer functions, *J. Hydrol.*, *251*(3–4), 163–176, doi:10.1016/S0022-1694(01)00466-8.
Scott, P. S., G. J. Farquhar, and N. Kouwen (1983), Hysteretic effects on net infiltration, in *Advances in Infiltration, Proceedings of the National Conference*, pp. 163–170, Am. Soc. of Agric. Eng., St. Joseph, Mich.
Šimůnek, J., M. T. van Genuchten, and M. Šejna (2008), Development and applications of the HYDRUS and STANMOD software packages and related codes, *Vadose Zone J.*, *7*(2), 587–600, doi:10.2136/vzj2007.0077.
Skierucha, W., A. Wilczek, A. Szypłowska, C. Sławiński, and K. Lamorski (2012a), A TDR-based soil moisture monitoring system with simultaneous measurement of soil temperature and electrical conductivity, *Sensors*, *12*(10), 13,545–13,566, doi:10.3390/s121013545.
Skierucha, W., A. Wilczek, and A. Szypłowska (2012b), Dielectric spectroscopy in agrophysics, *Int. Agrophys.*, *26*(2), 187–197, doi:10.2478/v10247-012-0027-5.
Sochan, A., A. Bieganowski, M. Ryżak, R. Dobrowolski, and P. Bartmiński (2012), Comparison of soil texture determined by two dispersion units of Mastersizer 2000, *Int. Agrophys.*, *26*(1), 99–102, doi:10.2478/v10247-012-0015-9.
Tartakovsky, D. M., and B. E. Wohlberg (2004), Delineation of geologic facies with statistical learning theory, *Geophys. Res. Lett.*, *31*, L18502, doi:10.1029/2004GL020864.
Tóth, B., A. Makó, A. Guadagnini, and G. Tóth (2012), Water retention of salt-affected soils: Quantitative estimation using soil survey information, *Arid Land Res. Manage.*, *26*(2), 103–121, doi:10.1080/15324982.2012.657025.
Tóth, B., M. Weynants, A. Nemes, A. Makó, G. Bilas, and G. Tóth (2015), New generation of hydraulic pedotransfer functions for Europe, *Eur. J. Soil Sci.*, *66*(1), 226–238, doi:10.1111/ejss.12192.
Trpkošová, D., and J. Mls (2010), Efficiency of capillary barriers in relation to retention curves data, *Acta Geodyn. Geomater.*, *7*(2), 201–207.
Twarakavi, N. K. C., J. Šimůnek, and M. G. Schaap (2009), Development of pedotransfer functions for estimation of soil hydraulic parameters using support vector machines, *Soil Sci. Soc. Am. J.*, *73*(5), 1443–1452.
van Dam, J. C., P. Groenendijk, R. F. A. Hendriks, and J. G. Kroes (2008), Advances of modeling water flow in variably saturated soils with SWAP, *Vadose Zone J.*, *7*(2), 640–653, doi:10.2136/vzj2007.0060.
van Genuchten, M. T. (1980), A closed-form equation for predicting the hydraulic conductivity of unsaturated soils, *Soil Sci. Soc. Am. J.*, *44*(5), 892–898.
Vapnik, V. N. (1995), *The Nature of Statistical Learning Theory*, Springer, New York.
Vereecken, H., J. Maes, J. Feyen, and P. Darius (1989), Estimating the soil moisture retention characteristic from texture, bulk density, and carbon content, *Soil Sci.*, *148*(6), 389–403.
Vereecken, H., J. Diels, and P. Viaene (1995), The effect of soil heterogeneity and hysteresis on solute transport: Numerical experiment, *Ecol. Modell.*, *77*(2–3), 273–288, doi:10.1016/0304-3800(94)00183-I.
Vereecken, H., et al. (2016), Modeling soil processes: Review, key challenges and new perspectives, *Vadose Zone J.*, *15*(5), doi:10.2136/vzj2015.09.0131.
Walczak, R. T., F. Moreno, C. Sławiński, E. Fernandez, and J. L. Arrue (2006), Modeling of soil water retention curve using soil solid phase parameters, *J. Hydrol.*, *329*(3–4), 527–533, doi:10.1016/j.jhydrol.2006.03.005.
Wohlberg, B., D. M. Tartakovsky, and A. Guadagnini (2006), Subsurface characterization with support vector machines, *IEEE Trans. Geosci. Remote Sens.*, *44*(1), 47–57, doi:10.1109/TGRS.2005.859953.
Wösten, J. H. M., A. Lilly, A. Nemes, C. Le Bas, J. H. M. Wosten, and H. Otto (1999), Development and use of a database of hydraulic properties of European soils, *Geoderma*, *90*(3–4), 169–185.
Zhou, A.-N. (2013), A contact angle-dependent hysteresis model for soil–water retention behaviour, *Comput. Geotech.*, *49*, 36–42, doi:10.1016/j.compgeo.2012.10.004.